



Published in final edited form as:

Biol Psychiatry. 2024 April 15; 95(8): 785–799. doi:10.1016/j.biopsych.2023.10.016.

Disengagement of somatostatin neurons from lateral septum circuitry by oxytocin and vasopressin restores social-fear extinction and suppresses aggression outbursts in Prader-Willi syndrome model

Yann Dromard^{1,*}, Amélie M. Borie^{1,*}, Prabahan Chakraborty^{1,*}, Françoise Muscatelli², Gilles Guillon¹, Michel G. Desarménien¹, Freddy Jeanneteau^{1,✉}

¹Institut de Génomique Fonctionnelle, University of Montpellier, INSERM, CNRS, France

²Institut de Neurobiologie de la Méditerranée, INSERM, University of Aix-Marseille, Marseille, France

Abstract

Background—Responding to social signals by expressing the correct behavior is not only challenged in autism, but also in diseases with high prevalence of autism, like Prader-Willi Syndrome (PWS). Clinical evidence suggests aberrant pro-social behavior in patients can be regulated by intranasal oxytocin (OXT) or vasopressin (AVP). However, what neuronal mechanisms underlie impaired behavioral responses in a socially-aversive context, and how can they be corrected, remains largely unknown.

Methods—Using the *Magel2* knocked-out (KO) mouse model of PWS (crossed with CRE-dependent transgenic lines), we devised optogenetic, physiological and pharmacological strategies in a social-fear-conditioning paradigm. Pathway specific roles of OXT and AVP signaling were investigated converging on the lateral septum (LS), a region which receives dense hypothalamic inputs.

Results—OXT and AVP signaling promoted inhibitory synaptic transmission in the LS, which failure in *Magel2*KO mice disinhibited somatostatin (SST) neurons and disrupted social-fear extinction. The source of OXT and AVP deficits mapped specifically in the supraoptic nucleus→LS pathway of *Magel2*KO mice disrupting social-fear extinction, which could be corrected by optogenetic or pharmacological inhibition of SST-neurons in the LS. Interestingly, LS SST-neurons also gated the expression of aggressive behavior, possibly as part of functional units operating beyond local septal circuits.

Conclusions—SST cells in the LS play a crucial role in integration and expression of disrupted neuropeptide signals in autism, thereby altering the balance in expression of safety versus fear.

✉ **Corresponding author:** freddy.jeanneteau@igf.cnrs.fr.

*Equal contribution

Author contributions

Conceptualization: FJ, AMB; Methodology: AMB, YD, FJ, PC, Investigations: AMB, YD, PC, FJ; Funding acquisition: FJ; Project administration and supervision: FJ; Writing—original draft: FJ, PC; Editing: FJ, PC, FM.

Disclosures

The authors have nothing to disclose and declare no competing interests.

Our results uncover novel mechanisms underlying dysfunction in a socially-aversive context, and provides a new framework for future treatments in autism-spectrum disorders.

Keywords

Autism; social-fear; aggression; extinction; lateral septum

Introduction

A key tenet of survival involves expressing context-appropriate behaviors, failing which gives rise to the symptomatology observed across many disease states. For instance, social deficits are well recorded across the autism spectrum disorders (ASD), including in subjects reporting deficiency of the *MAGEL2* gene and diagnosed with Prader-Willi syndrome (PWS) (1). PWS is a syndromic ASD (5–20% of cases) given its known clinical association with *MAGEL2* (2), and rare genetic disorder (1/10,000 – 1/25,000) that can be caused by a paternal deletion of the 15q11.2-q13 region containing the *MAGEL2* gene (65–75% of cases), maternal uniparental disomy (20–30% of cases), or an imprinting defect (1–3% of cases) (3). Mutated mice carrying only a single paternal copy of the *Magel2* gene - maternal copy being silent due to maternal imprinting (4)-exhibit a range of deficits including suckling deficiency as well as social impairments (5,6). While *Magel2KO* as a model of ASD may be underlined by the rarity of the disease, it is striking to note that the prevalence rate of *MAGEL2*-related ASD in PWS (25–84%) is well above the 1.5% reported in the general population (4,7). Syndromic autism as in PWS is also known to manifest in more severe ways than idiopathic ASD (8). *Magel2KO* mice thus sit at the interface of both ASD and PWS, recapitulating disease phenotypes in mouse and rat models (9). Studying *Magel2KO* mice in particular also adds the advantageous access to a genetic toolbox for investigating functional changes at cellular and circuit levels.

Aberrant social behaviour, as reported in *Magel2KO* mice, is expressed either as reduced pro-social behaviour or increased aggression. PWS patients show deficient social responses in positive contexts (1,10) as well as enhanced aggressiveness (11,12) and temper outbursts (13–16). Interestingly, two molecular players that are known to regulate pro-social and agonistic behaviors across species – oxytocin (OXT) and vasopressin (AVP) (17,18) – were found to be deficient in *MAGEL2*-deficient patient-derived cell lines (19). Furthermore, decreased levels of AVP and its pro-hormone convertase has been reported in the post-mortem hypothalamus of PWS patients (20). Some promising clinical trials with OXT report improved social behavior and trust in PWS (10). Intranasal AVP has also been found to be clinically effective in correcting social deficits in autism (21). Yet, variations in the therapeutic windows, the genetic heterogeneity between patients and the misunderstanding about the neuromodulatory effects of OXT and AVP on pro-social and agonistic behaviors could explain the inconsistent benefits in replicate studies (22–24). While this implies a crucial role of these hypothalamic neuropeptides in correcting pro-social deficits, their therapeutic role in treating aversive social experiences remains unexplored in PWS.

Impaired pro-social behavior has also been consistently reported in animal models of *Magel2*-deficiency (5,9), and linked to a post-natal mosaic expression of OXT-receptor

(25,26). Intervention with OXT and AVP also corrects pro-social deficits in *Mage12*KO mice (5,27). In wild-type (WT) animals, a role of OXT and AVP in social-fear and aggression has been revealed within the lateral septum (LS) (28–30) - a brain region where *Mage12* expression begins *in utero* (31). Receiving dense modulatory inputs of hypothalamic OXT and AVP neurons (30), studies report enhanced aggression arising from loss of neuropeptidergic support in the LS of WT animals (29,30). Still, it remains to be understood how OXT and AVP influence the function of LS neurons to regulate aggression in the syndromic autism of PWS.

To address this gap-in-knowledge, the present study in *Mage12*KO mice explores neuronal mechanisms within the LS using electrophysiological, optogenetic and pharmacological strategies, in a social-fear-conditioning paradigm (SFC) (32). While we have previously demonstrated neuropeptide-mediated reversal of pro-social deficits in this model (27), we now elucidate a novel framework which could be targeted for future therapeutic interventions, particularly to combat dysfunctional responses in an aversive context.

Methods

See Supplemental Methods and Materials for details.

Experiments were performed according to the Directive by the Council of the European Communities (86/609/EEC) following guidelines from French Ministry of research and ethics committee for the care and use of laboratory animals (approved protocols APAFIS-5133, 8940, 11468). All efforts were made to minimize animal suffering and reduce their number. All procedures were performed between 8:00 and 15:00-hr according to the ARRIVE guidelines.

Animals.

Age/weight-matched mice were group-housed under standard pathogen-free laboratory conditions (12/12 light/dark cycle, 22°C, 60% humidity, food and water *ad libitum*). *Oxt*-Cre (*Oxt*^{tm1.1(CRE)^{Dolsn}/J}), *Avp*-Cre (*Avp*^{tm1.1(cre)^{Hze}/J}), *Sst*-Cre (*Cg-Sst*^{tm2.1(cre)^{Zjh/Mwar}/J}) from Jackson labs and *Mage12*KO mice (*Mage12*^{tm1.1Mus/J}) were maintained under above conditions. *Mage12* gene is paternally (p) expressed and maternally (m) imprinted such that heterozygotes can be knockouts when the null allele is paternal (-p). All experiments were performed with heterozygote *Mage12*+m/-p mice as KO which show behavioural deficits as pups and parenting deficits as adults (25,33), and *Mage12*+m/+p mice as WT. Bodyweight was similar from weaning to sacrifice between WT and KO groups (Figure S1), with only an effect of age ($F_{(12, 55)} = 34,68$) but not genotype ($F_{(1, 13)} = 0,002364$). All lines were maintained for more than 10 generations in C57BL6 background, which has low levels of innate aggression (34,35). Although sexual dimorphism in septal neuropeptides systems requires gender-specific studies (30), here we used the social-fear paradigm in males, which had previously been mechanistically explored only in females (29,30).

Stereotaxy.

AAV1 EF1a::DIO-eNpHR3.0-eYFP;WPRE::hGH, EF1a::DIO-ChR2-eYFP;WPRE::hGH or EF1a::DIO-eYFP;WPRE::hGH (500nL, UPENN, USA) were used in this study. 6 weeks-

old *Oxt*-CRE, *Avp*-CRE or double transgenics with *Mage12*KO were injected in PVN (AP -0.9 mm, ML ± 0.2 mm, DV 4.5mm) or SON (AP -5.6 mm, ML ± 1.13 mm, DV -5.45 mm). *Sst*-CRE mice were injected in LS (AP $+0.3$ mm, ML ± 0.3 mm, DV -2.5 mm). Bilateral fibers (Doric lenses, 0.53NA) were implanted at the same coordinates and verified postmortem. *See supplemental methods for stimulation details, recombination efficiency.*

Intracerebral infusions.

See supplemental methods.

Social-fear conditioning.

A week before testing, males (3–4 months old) were habituated to the experimenter and isolated (cage $27 \times 22 \times 14$ cm). The conditioning arena was a transparent Plexiglas chamber ($22 \times 30 \times 44$ cm) with an electric grid floor, cleaned with detergent. Following habituation to the arena, the conditioned mouse received footshocks (0.6 mA, 2s) upon each social contact with an unfamiliar stimulus mouse. A single foot-shock was given upon each social contact (5 footshocks in total), and conditioned mice were returned to their homecage when no further social contact was made in the 3 min after the last shock (32). *See supplemental methods for average number of footshocks/group.*

Social-fear extinction.

On day 2, mice were presented with the stimulus box containing objects (3-times) or distinct unfamiliar conspecifics (6-times) in their homecage for 3 min each, with a 3 min inter-stimulus-interval. Successful discrimination was defined as exploring the sixth unfamiliar mouse 20% more time than the first. On day 3, mice were exposed once to a new stimulus mouse to assess fear extinction memory.

Aggression.

As shown in supplemental video-1, aggressive behaviours were marked by repeated attacks towards and biting of the stimulus mice through the grid of the stimulus box. Total duration, number of attacks and latency of first attack were scored during extinction.

Patch clamp.

Acute slices were prepared and maintained as previously described (27), and LS neurons were visualized and randomly recorded from the dorsolateral septum (Figure S2) using Normarsky contrast microscopy. TGOT (0.1 μ M)/AVP (1 μ M) were bath-applied (2 min) and washed with ACSF (minimum 20 min) to return to baseline activity. AMPAR-antagonist CNQX (1 μ M)/GABA_A-R-antagonist GABazine (1 μ M) was bath-applied during the entire period with TGOT/AVP to test for glutamate-mediated and GABA-mediated currents. The sodium channel blocker TTX (0.3 μ M) was bath-applied during the entire period with TGOT/AVP to test for spontaneous network activity on synaptic transmission. Data was acquired at 10 kHz sampling rate through and processed with Clampfitv9 (Molecular Devices). *See supplemental methods and Figure S3 for opsin activity verification.*

Histology.

See supplemental methods.

Statistics.

Data presented as means±SEM were analyzed with Prism 9 (GraphPad, La Jolla, CA). Normally distributed data (Shapiro-Wilk and Kolmogorov-Smirnov tests) were tested with parametric two-sided t-test for pairwise and ANOVA for multiple comparisons. Otherwise, non-parametric Mann-Whitney and Wilcoxon tests were used for two-sided unpaired and paired comparisons, respectively. Differential proportions were determined with Chi². N and statistical tests are indicated in figures and legends. Significance reported as follows: * $p<0.05$, ** $p<0.001$, *** $p<0.0001$.

Results

***Magel2*KO mice show impaired extinction of a social-fear memory**

To explore the social aversive circuitry involving OXT and AVP networks, *Magel2*WT and *Magel2*KO mice were trained to fear social contacts with unknown conspecifics (same sex and age) by using electrical footshocks (SFC+) (Figure 1A). There was no effect of genotype on the reactivity to the strength and duration of shocks (Figure S4). Twenty-four hours later, this was followed by re-exposure to unknown mice over 6 trials in absence of footshocks in its homecage (Figure 1A). SFC+ subjects explored the new conspecific less in the earlier trials (Stimulus-mouse 1), although improving later (Stimulus-mouse 6) (Figure 1B). Quantitatively, WT SFC+ subjects showed a gradual extinction of social-fear (Figure 1D), with social exploration comparable to unconditioned SFC– mice by trial 6 (Figure 1C). In contrast, SFC+ *Magel2*KO mice failed to fully extinguish the acquired fear (Figure 1D). Both groups showed no fear to objects (Figure 1E,F) implying the fear memory was social-specific. Moreover, a significantly less proportion of *Magel2*KO mice failed to successfully discriminate stimulus mice between the first and last trials (Figure 1G), and memory deficits persisted when recall was tested with an unfamiliar conspecific on day 3 (Figure 1H). Both learning (Figure 1I) and number of footshocks delivered during conditioning (~2 in 3 min) were similar across groups. Together, these results indicate that *Magel2*KO mice have difficulties in social-fear extinction, and thus fail to discriminate between social-fear and safety.

Impaired social circuitry in *Magel2*KO mice

To investigate the neural networks underlying behavioral deficits in *Magel2*KO mice, we counterstained Fos-labeled neurons with neurophysin antibodies in SFC+ and SFC– mice (Figure 2A). In WT mice, differential expression of c-Fos in the AVP and OXT neurons of the paraventricular nuclei (PVN) was more pronounced during conditioning than extinction. By contrast, it was the AVP and OXT neurons of the supraoptic nuclei (SON) that were prominently engaged during extinction (Figure 2B,C). Given that *Magel2*KO mice showed deficits of extinction rather than acquisition, we analyzed the expression of c-Fos in both nuclei on day 2. Interestingly, engagement of these cells was significantly attenuated in *Magel2*KO mice (Figure 2B,C). Thus, while both peptidergic neuron types are required for

social-fear extinction learning, preferential activation of the SON is robustly hampered in *Magel2*KO mice.

Next, we backcrossed *Magel2*KO mice with either *Avp*-CRE or *Oxt*-CRE animals to understand the functional consequence of this loss. Adeno-associated viruses (AAV) to express CRE-dependent transgenes were bilaterally injected in either hypothalamic nuclei of *Avp*-CRE and *Oxt*-CRE mice. Optic fibers were implanted in LS, which receives heavy hypothalamic projections (Figure 3A) involved in both pro-social and agonistic behaviors (36). Robust recombination was detected in both PVN (Figure 3B) and SON (Figure 3E), with axonal projections detected in LS (Figure 3A). In WT mice, stimulation of NpHR3 in the vasopressinergic PVN→LS fibers (Figure 3C) or the oxytocinergic PVN→LS fibers (Figure 3D) with continuous yellow light had no effect on social-fear extinction. In contrast, silencing SON→LS fibers of AVP (Figure 3F) or OXT neurons (Figure 3G) with NpHR3 in WT subjects impaired social-fear extinction, agreeing with the Fos-mapping data. Such inhibition of SON-fibers also promoted aggressive behaviors, marked by greater amount of time spent in biting/repeatedly attacking the stimulus mice (Figure 3H), higher number of such attacks (Figure S5A) and a reduced latency for the first attack (Figure S6A). Neither WT nor *Magel2*KO mice were aggressive at baseline (WT 1.9 ± 0.9 s, KO 0.3 ± 0.2 s).

Lastly, to confront the loss of peptides in the LS of *Magel2*KO mice, we expressed ChR2-eYFP (or eYFP as control) in the PVN (Figure 3J) or SON (Figure 3M), and optogenetically activated either projection in LS with pulsed blue light. Activating OXT (Figure 3K) or AVP fibers (Figure 3L) from PVN→LS had no effect on extinction in SFC+ subjects. In contrast, optogenetic activation of the AVP (Figure 3N) or OXT (Figure 3O) fibers from the SON promoted extinction learning in conditioned *Magel2*KO mice. Taken together, the gain- and loss-of-function experiments determined that both peptides secreted from the SON contribute to the expression of social safety by facilitating social discrimination in an aversive context (Figure 3I).

AVP and OXT promote inhibitory synaptic transmission in the LS

To understand how *Magel2* loss impacts downstream effects of hypothalamic neuropeptides in LS, we recorded synaptic events in LS in response to AVP and TGOT, a selective OXTR-agonist (Figure 4). Whole-cell patch clamp unveiled two major types of synaptic transmission - bursting events (40%, duration: 3–39s, frequency: 4.2 Hz), interspaced by silences (60%, duration: 2–82s) (Figure 4A). We fixed the intracellular chloride concentration to set the inversion potential E_{Cl} at -45 mV and recorded at -80 mV. Depolarization steps transformed most inward currents into outward currents at $E_{Cl} = -45$ mV, suggesting that synaptic events must be inhibitory (Figure 4B). Indeed, GABA-A antagonist GABAzine blocked these events in a significant population of cells (type-1), while some cells remained partially affected (type-2), suggesting the possibility of excitatory events (Figure 4C). To distinguish between the inversion potential of glutamatergic currents $E_{Na/K}$ and GABAergic currents E_{Cl} , we artificially set E_{Cl} at -80 mV, $E_{Na/K}$ at 0 mV, and recorded at -45 mV the frequency of inward excitatory synaptic currents (EPSC) and outward inhibitory synaptic currents (IPSC). As expected, type-1 cells responded very little to bath application of glutamate receptors antagonist CNQX, suggesting paucity

of excitatory inputs, while the frequency was increased in type-2 cells - indicating the presence of excitatory inputs (Figure 4D). Proportionally, 2/3 of all events in the type-1 cells were GABA-ergic (Figure 4E). Next, bath application of AVP and TGOT modified IPSC frequency in type-1 (Figure 4F,G), but not in type-2 cells (Figure 4H). GABA_A and Na⁺-channel blocker TTX blocked these effects (Figure 4I), indicating that both peptides promote inhibitory synaptic transmission in local networks. Contrastingly, AVP and TGOT had no effect on excitatory post-synaptic currents (EPSC) in the type-1 cells (Figure 4J), and only AVP stimulated EPSC in the type-2 cells (Figure 4K). Finally, application of AVP and TGOT triggered typical IPSC and EPSC responses in slices of *Magel2*KO mice, except that *Magel2*KO mice lacked a majority of cells with the type-1 profile. This indicates an over-representation of type-2 cells in the LS of *Magel2*KO as compared to WT-controls (Figure 4L).

SST-neurons in the LS of *Magel2*KO mice are disinhibited

To identify the type-1 cells misrepresented in *Magel2*KO LS, we injected a fluorescent tracer into the patch pipette and counterstained with several protein markers. A majority of type-1 cells stained for somatostatin (SST) (Figure 5A,B). Next, we examined co-expression of specific receptors for AVP (AVPR) and OXT (OXTR). We recently developed a fluorescent peptide to detect AVPR binding sites, when OXTR are blocked with a specific competitive ligand (27) (Figure 5C). This fluorescent peptide marked SST-neurons (Figure 5D) but only 1/3 of them (Figure 5E). In contrast, 2/3 of SST-neurons in the LS co-labeled with OXTR binding sites when AVPRs were blocked with a specific competitive ligand (Figure 5F,G). Could these SST cells be engaged during social-fear extinction? Indeed, a significantly higher proportion of SST-neurons were fos-activated in *Magel2*KO mice during recall (Figure 5H,I), suggesting their over-activation due to lack of inhibition by neuropeptide signaling.

How would these SST-neurons regulate fear extinction and aggression in *Magel2*KO mice? We injected AAV virus in LS of *SST*-CRE mice crossed with *Magel2*KO to express DIO-NpHR3-eYFP or DIO-eYFP as control (Figure 6A). Consistent with fos-mapping, optogenetic silencing of LS SST-neurons with continuous yellow light promoted social-fear extinction as compared to eYFP controls (Figure 6B). This improved discrimination in a majority of *Magel2*KO mice (Figure 6C) without triggering aggression (Figure 6D, S5B and S6B). Conversely, we tested if SST neuron activation was sufficient to trigger an extinction deficit, by injecting DIO-ChR2-eYFP in the LS of WT animals. Indeed, pulsed-blue light activation of SST-neurons significantly impaired social-fear extinction in WT (Figure 6F), with a significant proportion failing to discriminate (Figure 6G) and expressing aggression (Figure 6H, S5C, and S6C). In sum, these approaches imply an overactivation of LS SST-neurons, thus impairing social-fear extinction and triggering aggressive behaviors.

SSTR in LS control social-fear extinction but not aggression

Despite an over engagement of LS SST-positive type-1 neurons, *Magel2*KO mice are not aggressive at baseline – indicating that distinct local or long-distance SST circuitries in the septum may be regulating social-fear extinction vs. aggression (36). To distinguish between these two possibilities, we pharmacologically targeted SST receptors (SSTR) within the LS.

Injection of fluorescent beads through implanted bilateral cannulas validated local diffusion (Figure 7A). Next, intra-LS injection of pan-SSTR antagonist cyclosomatostatin during extinction learning improved social exploration (Figure 7B) and discrimination (Figure 7C) in *Magel2*KO mice as compared to NaCl-injected KO-controls, without affecting aggression (Figure 7D, S5D and S6D). By contrast, injecting SSTR peptide agonist SST14 in the LS of *Magel2*WT mice during extinction not only impaired extinction (Figure 7E) but also discrimination (Figure 7F), with a non-significant trend for aggressive behaviour (Mann-Whitney test $p=0.06$) (Figure 7G and S5E, S6E). Such pharmacological overactivation suggests local SSTR signaling in LS selectively regulates social-fear extinction, while recapitulating mutant deficits in WT mice.

Discussion

The present study examined neuronal mechanisms of aberrant social-fear in a mouse model of PWS. We first report that *Magel2*KO mice failed to extinguish a previously acquired social-fear memory. This lies in agreement with clinical studies reporting social-fear in *Magel2*-deficient patients (37) and elevated distress to social but not non-social cues in autistic toddlers (38). This possibly arises from an inability to recognize negative emotions (39), and could underlie comorbid social anxiety seen in many autistic subjects, including PWS patients (40–42). In *Magel2*KO animals, deficits in pro-social behavior have been well-reported (9,27,43), although non-social-fear memory was found to be unaffected (9,44). We report for the first time that *Magel2*KO animals had difficulties to extinguish fear memories in a social context.

To improve social behavior in autism, intranasal OXT has been found to enhance orientation towards affective images (45) and increase social salience (46) in autistic subjects. Recently, intranasal AVP has also been found to improve social behavior in autism (21). We have recently demonstrated that in *Magel2*KO mice, a lack of AVP from BNST failed to inhibit LS SST-neurons, impairing within-session discrimination of a novel juvenile mouse (27). Intra-septal AVP-injections as well as stimulation of vasopressinergic BNST→LS fibers prevented this. Additionally, we noticed no aggression, supporting a pivotal role of septal AVP in social behaviour unrelated to social memory or aggression. Furthermore, hypothalamic OXT cells in *Magel2*KO mice show reduced spiking frequency of EPSCs and increased NMDA/AMPA ratio, indicating a weakened neuropeptidergic system (47). Consistent with these findings, we not only observed reduced OXT/AVP engagement in the present study, but also found a strikingly preferential weakening of SON→LS pathway in extinction-resistant *Magel2*KO mice. Previous studies in lactating female rats report that SON→LS OXT release prevents social-fear, while in virgins, lack of OXT in LS disrupts social-fear extinction (29) similar to our observations in males. An intra-LS circuit also modulates aggression in female rats, wherein increased OXT in ventral-LS and low AVP in the dorsal-LS promotes aggression by suppressing putative SST-neurons (30). While we observed enhanced aggression with both low AVP and OXT that impinged on SST-neurons of male mice, how neuropeptide crosstalk within LS might influence this remains to be seen in males.

Downstream of neuropeptide signaling, we identified hyperactivated OXT-receptor expressing SST-neurons in the LS of mutant mice, which poorly regulated fear extinction. Not just neuropeptide loss, even OXT receptors are dysregulated post-natally in *Magel2*KO animals (25), which are key to social learning in both rewarding and aversive contexts (48). Central amygdala OXT is involved in discrimination of conspecifics' emotional states (49), while blocking OXTR in LS prevents social-fear extinction, and intra-LS OXT infusion facilitates the same (50) - in agreement with our findings in *Magel2*KO. We add that this acts via SST-neurons, which in the prefrontal cortex are significantly activated during expression of social-fear (51), and in the central amygdala promote passive defensive behaviours following fear learning (52). Within the LS, activity of foot-shock responsive SST-neurons correlates with non-freezing bouts during contextual fear recall, such that silencing them increases freezing (53). In light of our observations, we infer that LS SST-neurons might regulate a change of behavioural state, maintaining the balance between expression of fear extinction and aggression.

It is tempting to speculate the above mutually-exclusive behaviours are perhaps regulated by discrete 'functional units' in the LS, wherein interacting septal neurons work in tandem as a unit to express one behavior or the other (36). Based on our observations, we propose a model with septal SST-neurons forming half of such a putative functional unit, regulating social-fear while gating aggression (Figure 8). Selectively AVP-responsive type-2 neurons that we characterized may form the other half, controlling aggression-circuits and gating extinction. At baseline in WT, type-2 cells would inhibit SST-neurons, rendering them unresponsive to OXT, while maintaining inhibitory control over aggression circuits, thereby facilitating extinction without affecting aggression. Arresting OXT-release with halorhodopsin allows SST-neurons to exert stronger inhibition over type-2 neurons - leading to impaired extinction and high aggression. By contrast, preventing AVP-release would weaken the inhibitory control of type-2 over SST-neurons, leading to the same outcome. This aligns with previous reports suggesting that a lack of neuropeptide support in the LS triggers aggressive behaviours (28,54,55). Conversely, optogenetic stimulation of SST-neurons in WT mice would allow it to exert a stronger inhibition on type-2 cells, and so social-fear extinction would be impaired and aggression circuits disinhibited and expressed - as we observe.

In *Magel2*KO mice, on the other hand, a global lack of neuropeptide signaling means that SST and type-2 cells would *both* be strengthened, thus inhibiting each other as well as preventing expression of *both* social-fear extinction and aggression - explaining the lack of aggression seen at baseline in *Magel2*KO mice. Tilting the balance of this functional unit in *Magel2*KO mice by opto-silencing the SST cells would only disinhibit and facilitate fear extinction, sparing aggression. Pharmacological manipulations with SST agonism/antagonism in this study argue in favor of such a local functional unit in the septum specifically governing fear extinction. Beyond local SSTR-mediated signaling, aggression could be regulated by ventromedial hypothalamus-projecting neurons in the LS, perhaps forming the downstream targets of other half of the proposed functional unit (36,56).

While increased activity of LS SST-neurons has been typically involved with fear and anxiety (53), blunted function of deep-seated *Drd3*⁺ septal neurons in stress-exposed mice

impair social interaction (36,57). Septal dopamine release is involved in aggression too (58) – suggesting that *Drd3+* neurons may form the other half of the putative functional unit. Interestingly, increased activity of neurotensin+ (59), *Crf2+* (60) and vGAT+ (61) cells in the LS also favour aversive behavioural outcomes. Could the modulatory effects of social neuropeptides like AVP and OXT then be mediated by an overlapping subset of cells? It seems unlikely, given that in the LS, we have previously demonstrated a predominant neuropeptide binding to SST-neurons (27). Hence despite a functional heterogeneity in the septum, we believe that non-overlapping SST-neurons in the LS principally govern the selective behavioral outcomes observed at the intersection of *Mage12*-deficiency and social-fear.

In sum, we unravel a pivotal role of septal SST-neurons to regulate the balance between social-fear and aggression in *Mage12*KO mice, located downstream of a pathway-specific loss in neuropeptide control. This not only proposes somatostatin as a novel target in PWS, but also provides a new framework to consider its integrative role in combination with existing neuropeptide therapies, in the treatment of neurodevelopmental and intellectual disabilities.

Supplementary Material

Refer to Web version on PubMed Central for supplementary material.

Acknowledgments

We thank H. Gainer (NIH, USA) for antibodies. Funding agencies are Agence Nationale pour la Recherche PRC (FM), and Fondation pour la Recherche Médicale (FJ). We also thank D Huzard for setting up the social-fear-conditioning task.

References

1. Dimitropoulos A, Ho A, Feldman B. Social Responsiveness and Competence in Prader-Willi Syndrome: Direct Comparison to Autism Spectrum Disorder. *J Autism Dev Disord*. 2013 Jan;43(1):103–13. [PubMed: 22576167]
2. Schaaf CP, Gonzalez-Garay ML, Xia F, Potocki L, Gripp KW, Zhang B, et al. Truncating mutations of MAGEL2 cause Prader-Willi phenotypes and autism. *Nat Genet*. 2013 Nov;45(11):1405–8. [PubMed: 24076603]
3. Dykens EM, Roof E, Hunt-Hawkins H, Dankner N, Lee EB, Shivers CM, et al. Diagnoses and characteristics of autism spectrum disorders in children with Prader-Willi syndrome. *J Neurodevel Disord*. 2017 Dec;9(1):18.
4. Fountain M, Schaaf C. Prader-Willi Syndrome and Schaaf-Yang Syndrome: Neurodevelopmental Diseases Intersecting at the MAGEL2 Gene. *Diseases*. 2016 Jan 13;4(1):2. [PubMed: 28933382]
5. Meziane H, Schaller F, Bauer S, Villard C, Matarazzo V, Riet F, et al. An Early Postnatal Oxytocin Treatment Prevents Social and Learning Deficits in Adult Mice Deficient for *Mage12*, a Gene Involved in Prader-Willi Syndrome and Autism. *Biological Psychiatry*. 2015 Jul;78(2):85–94. [PubMed: 25599930]
6. Schaller F, Watrin F, Sturny R, Massacrier A, Szepetowski P, Muscatelli F. A single postnatal injection of oxytocin rescues the lethal feeding behaviour in mouse newborns deficient for the imprinted *Mage12* gene. *Human Molecular Genetics*. 2010 Dec 15;19(24):4895–905. [PubMed: 20876615]

7. Kong X, Zhu J, Tian R, Liu S, Sherman HT, Zhang X, et al. Early Screening and Risk Factors of Autism Spectrum Disorder in a Large Cohort of Chinese Patients With Prader-Willi Syndrome. *Front Psychiatry*. 2020 Nov 26;11:594934. [PubMed: 33329146]
8. Sztainberg Y, Zoghbi HY. Lessons learned from studying syndromic autism spectrum disorders. *Nat Neurosci*. 2016 Nov;19(11):1408–17. [PubMed: 27786181]
9. Reznik DL, Yang MV, Albelda De La Haza P, Jain A, Spanjaard M, Theiss S, et al. Magel2 truncation alters select behavioral and physiological outcomes in a rat model of Schaaf-Yang syndrome. *Disease Models & Mechanisms*. 2023 Feb 1;16(2):dmm049829. [PubMed: 36637363]
10. Oztan O, Zyga O, Stafford DEJ, Parker KJ. Linking oxytocin and arginine vasopressin signaling abnormalities to social behavior impairments in Prader-Willi syndrome. *Neuroscience & Biobehavioral Reviews*. 2022 Nov;142:104870. [PubMed: 36113782]
11. Rice LJ, Gray KM, Howlin P, Taffe J, Tonge BJ, Einfeld SL. The developmental trajectory of disruptive behavior in Down syndrome, fragile X syndrome, Prader-Willi syndrome and Williams syndrome. *Am J Med Genet*. 2015 Jun;169(2):182–7. [PubMed: 25983069]
12. Singh D, Wakimoto Y, Filangieri C, Pinkhasov A, Angulo M. Guanfacine Extended Release for the Reduction of Aggression, Attention-Deficit/Hyperactivity Disorder Symptoms, and Self-Injurious Behavior in Prader-Willi Syndrome—A Retrospective Cohort Study. *Journal of Child and Adolescent Psychopharmacology*. 2019 May;29(4):313–7. [PubMed: 30724590]
13. Tunnicliffe P, Woodcock K, Bull L, Oliver C, Penhallow J. Temper outbursts in Prader-Willi syndrome: causes, behavioural and emotional sequence and responses by carers: Temper outbursts in Prader-Willi syndrome. *J Intellect Disabil Res*. 2014 Feb;58(2):134–50. [PubMed: 23374136]
14. Rice LJ, Lagopoulos J, Brammer M, Einfeld SL. Reduced gamma-aminobutyric acid is associated with emotional and behavioral problems in Prader-Willi syndrome. *Am J Med Genet*. 2016 Dec;171(8):1041–8. [PubMed: 27338833]
15. Rice LJ, Lagopoulos J, Brammer M, Einfeld SL. Microstructural white matter tract alteration in Prader-Willi syndrome: A diffusion tensor imaging study. *Am J Med Genet*. 2017 Sep;175(3):362–7. [PubMed: 28834083]
16. Rice LJ, Woodcock K, Einfeld SL. The characteristics of temper outbursts in Prader-Willi syndrome. *Am J Med Genet*. 2018 Nov;176(11):2292–300. [PubMed: 30289600]
17. Young LJ. Oxytocin and Vasopressin Receptors and Species-Typical Social Behaviors. *Hormones and Behavior*. 1999 Dec;36(3):212–21.
18. Keverne EB, Curley JP. Vasopressin, oxytocin and social behaviour. *Current Opinion in Neurobiology*. 2004 Dec;14(6):777–83. [PubMed: 15582383]
19. Chen H, Victor AK, Klein J, Tacer KF, Tai DJC, De Esch C, et al. Loss of MAGEL2 in Prader-Willi syndrome leads to decreased secretory granule and neuropeptide production. *JCI Insight*. 2020 Sep 3;5(17):e138576. [PubMed: 32879135]
20. Attenuation of the Polypeptide 7B2, Prohormone Convertase PC2, and Vasopressin in the Hypothalamus of Some Prader-Willi Patients: Indications for a Processing Defect.
21. Parker KJ, Oztan O, Libove RA, Mohsin N, Karhson DS, Sumiyoshi RD, et al. A randomized placebo-controlled pilot trial shows that intranasal vasopressin improves social deficits in children with autism. *Sci Transl Med*. 2019 May 8;11(491):eaau7356. [PubMed: 31043522]
22. Ooi Y, Weng SJ, Kossowsky J, Gerger H, Sung M. Oxytocin and Autism Spectrum Disorders: A Systematic Review and Meta-Analysis of Randomized Controlled Trials. *Pharmacopsychiatry*. 2016 Aug 30;50(01):5–13. [PubMed: 27574858]
23. Bolognani F, Del Valle Rubido M, Squassante L, Wandel C, Derks M, Murtagh L, et al. A phase 2 clinical trial of a vasopressin V1a receptor antagonist shows improved adaptive behaviors in men with autism spectrum disorder. *Sci Transl Med*. 2019 May 8;11(491):eaat7838. [PubMed: 31043521]
24. Anpilov S, Shemesh Y, Eren N, Harony-Nicolas H, Benjamin A, Dine J, et al. Wireless Optogenetic Stimulation of Oxytocin Neurons in a Semi-natural Setup Dynamically Elevates Both Pro-social and Agonistic Behaviors. *Neuron*. 2020 Aug;107(4):644–655.e7. [PubMed: 32544386]
25. Gigliucci V, Busnelli M, Santini F, Paolini C, Bertoni A, Schaller F, et al. Oxytocin receptors in the Magel2 mouse model of autism: Specific region, age, sex and oxytocin treatment effects. *Front Neurosci*. 2023 Mar 14;17:1026939. [PubMed: 36998737]

26. Bertoni A, Schaller F, Tyzio R, Gaillard S, Santini F, Xolin M, et al. Oxytocin administration in neonates shapes hippocampal circuitry and restores social behavior in a mouse model of autism. *Mol Psychiatry*. 2021 Dec;26(12):7582–95. [PubMed: 34290367]
27. Borie AM, Dromard Y, Guillon G, Olma A, Manning M, Muscatelli F, et al. Correction of vasopressin deficit in the lateral septum ameliorates social deficits of mouse autism model. *Journal of Clinical Investigation*. 2021 Jan 19;131(2):e144450. [PubMed: 33232306]
28. Veenema AH, Beiderbeck DI, Lukas M, Neumann ID. Distinct correlations of vasopressin release within the lateral septum and the bed nucleus of the stria terminalis with the display of intermale aggression. *Hormones and Behavior*. 2010 Jul;58(2):273–81. [PubMed: 20298693]
29. Menon R, Grund T, Zoicas I, Althammer F, Fiedler D, Biermeier V, et al. Oxytocin Signaling in the Lateral Septum Prevents Social Fear during Lactation. *Current Biology*. 2018 Apr;28(7):1066–1078.e6. [PubMed: 29551417]
30. Oliveira VEDM, Lukas M, Wolf HN, Durante E, Lorenz A, Mayer AL, et al. Oxytocin and vasopressin within the ventral and dorsal lateral septum modulate aggression in female rats. *Nat Commun*. 2021 May 18;12(1):2900. [PubMed: 34006875]
31. Kozlov SV, Bogenpohl JW, Howell MP, Wevrick R, Panda S, Hogenesch JB, et al. The imprinted gene *Magel2* regulates normal circadian output. *Nat Genet*. 2007 Oct;39(10):1266–72. [PubMed: 17893678]
32. Toth I, Neumann ID, Slattery DA. Social Fear Conditioning: A Novel and Specific Animal Model to Study Social Anxiety Disorder. *Neuropsychopharmacol*. 2012 May;37(6):1433–43.
33. Higgs MJ, Webberley AE, John RM, Isles AR. Parenting deficits in *Magel2*-null mice predicted from systematic investigation of imprinted gene expression in galanin neurons of the hypothalamus [Internet]. *Neuroscience*; 2023 Mar [cited 2023 Aug 7]. Available from: <http://biorxiv.org/lookup/doi/10.1101/2023.03.27.534088>
34. Weber EM, Zidar J, Ewaldsson B, Askevik K, Udén E, Svensk E, et al. Aggression in Group-Housed Male Mice: A Systematic Review. *Animals*. 2022 Dec 30;13(1):143. [PubMed: 36611751]
35. Nicholson A, Malcolm RD, Russ PL, Cough K, Touma C, Palme R, et al. The Response of C57BL/6J and BALB/cJ Mice to Increased Housing Density. *Journal of the American Association for Laboratory Animal Science*. 2009;48(6).
36. Besnard A, Leroy F. Top-down regulation of motivated behaviors via lateral septum sub-circuits. *Mol Psychiatry*. 2022 Aug;27(8):3119–28. [PubMed: 35581296]
37. Duan Y, Liu L, Zhang X, Jiang X, Xu J, Guan Q. Phenotypic spectrum and mechanism analysis of Schaff Yang syndrome: A case report on new mutation of *MAGEL2* gene. *Medicine*. 2021 Jun 18;100(24):e26309. [PubMed: 34128869]
38. Macari SL, Verneti A, Chawarska K. Attend Less, Fear More: Elevated Distress to Social Threat in Toddlers With Autism Spectrum Disorder. *Autism Research* 2021 May;14(5):1025–36. [PubMed: 33283976]
39. Uljarevic M, Hamilton A. Recognition of Emotions in Autism: A Formal Meta-Analysis. *J Autism Dev Disord*. 2013 Jul;43(7):1517–26. [PubMed: 23114566]
40. Capriola NN, Maddox BB, White SW. No Offense Intended: Fear of Negative Evaluation in Adolescents and Adults with Autism Spectrum Disorder. *J Autism Dev Disord*. 2017 Dec;47(12):3803–13. [PubMed: 27324492]
41. Maddox BB, White SW. Comorbid Social Anxiety Disorder in Adults with Autism Spectrum Disorder. *J Autism Dev Disord*. 2015 Dec;45(12):3949–60. [PubMed: 26243138]
42. Forster JL, Gourash LM. Managing Prader-Willi Syndrome: A Primer for Psychiatrists. 2005;
43. Fountain MD, Tao H, Chen CA, Yin J, Schaaf CP. *Magel2* knockout mice manifest altered social phenotypes and a deficit in preference for social novelty: Behavioral phenotyping of *Magel2* deficient mice. *Genes, Brain and Behavior*. 2017 Jul;16(6):592–600. [PubMed: 28296079]
44. Mercer RE, Kwolek EM, Bischof JM, Van Eede M, Henkelman RM, Wevrick R. Regionally reduced brain volume, altered serotonin neurochemistry, and abnormal behavior in mice null for the circadian rhythm output gene *Magel2*. *Am J Med Genet*. 2009 Dec 5;150B(8):1085–99. [PubMed: 19199291]

45. Althaus M, Groen Y, Wijers AA, Noltes H, Tucha O, Hoekstra PJ. Oxytocin enhances orienting to social information in a selective group of high-functioning male adults with autism spectrum disorder. *Neuropsychologia*. 2015 Dec;79:53–69. [PubMed: 26498227]
46. Domes G, Heinrichs M, Kumbier E, Grossmann A, Hauenstein K, Herpertz SC. Effects of Intranasal Oxytocin on the Neural Basis of Face Processing in Autism Spectrum Disorder. *Biological Psychiatry*. 2013 Aug;74(3):164–71. [PubMed: 23510581]
47. Ates T, Oncul M, Dilsiz P, Topcu IC, Civas CC, Alp MI, et al. Inactivation of Magel2 suppresses oxytocin neurons through synaptic excitation-inhibition imbalance. *Neurobiology of Disease*. 2019 Jan;121:58–64. [PubMed: 30240706]
48. Choe HK, Reed MD, Benavidez N, Montgomery D, Soares N, Yim YS, et al. Oxytocin Mediates Entrainment of Sensory Stimuli to Social Cues of Opposing Valence. *Neuron*. 2015 Jul;87(1):152–63. [PubMed: 26139372]
49. Ferretti V, Maltese F, Contarini G, Nigro M, Bonavia A, Huang H, et al. Oxytocin Signaling in the Central Amygdala Modulates Emotion Discrimination in Mice. *Current Biology*. 2019 Jun;29(12):1938–1953.e6. [PubMed: 31178317]
50. Zoicas I, Slattery DA, Neumann ID. Brain Oxytocin in Social Fear Conditioning and Its Extinction: Involvement of the Lateral Septum. *Neuropsychopharmacol*. 2014 Dec;39(13):3027–35.
51. Xu H, Liu L, Tian Y, Wang J, Li J, Zheng J, et al. A Disinhibitory Microcircuit Mediates Conditioned Social Fear in the Prefrontal Cortex. *Neuron*. 2019 May;102(3):668–682.e5. [PubMed: 30898376]
52. Yu K, Garcia Da Silva P, Albeanu DF, Li B. Central Amygdala Somatostatin Neurons Gate Passive and Active Defensive Behaviors. *J Neurosci*. 2016 Jun 15;36(24):6488–96. [PubMed: 27307236]
53. Besnard A, Gao Y, TaeWoo Kim M, Twarkowski H, Reed AK, Langberg T, et al. Dorsolateral septum somatostatin interneurons gate mobility to calibrate context-specific behavioral fear responses. *Nat Neurosci*. 2019 Mar;22(3):436–46. [PubMed: 30718902]
54. Compaan JC, Buijs RM, Pool CW, De Ruiter AJH, Koolhaas JM. Differential lateral septal vasopressin innervation in aggressive and nonaggressive male mice. *Brain Research Bulletin*. 1993 Jan;30(1–2):1–6. [PubMed: 8420617]
55. Oxytocin: the neurochemical mediator of social life: a pharmaco-behavioral and neurobiological study in male rats. Groningen: University of Groningen; 2014.
56. Leroy F, Park J, Asok A, Brann DH, Meira T, Boyle LM, et al. A circuit from hippocampal CA2 to lateral septum disinhibits social aggression. *Nature*. 2018 Dec;564(7735):213–8. [PubMed: 30518859]
57. Shin S, Pribrag H, Lilascharoen V, Knowland D, Wang XY, Lim BK. Drd3 Signaling in the Lateral Septum Mediates Early Life Stress-Induced Social Dysfunction. *Neuron*. 2018 Jan;97(1):195–208.e6. [PubMed: 29276054]
58. Mahadevia D, Saha R, Manganaro A, Chuhma N, Ziolkowski-Blake A, Morgan AA, et al. Dopamine promotes aggression in mice via ventral tegmental area to lateral septum projections. *Nat Commun*. 2021 Nov 23;12(1):6796. [PubMed: 34815379]
59. Li L, Durand-de Cuttoli R, Aubry AV, Burnett CJ, Cathomas F, Parise LF, et al. Social trauma engages lateral septum circuitry to occlude social reward. *Nature*. 2023 Jan 26;613(7945):696–703. [PubMed: 36450985]
60. Anthony TE, Dee N, Bernard A, Lerchner W, Heintz N, Anderson DJ. Control of Stress-Induced Persistent Anxiety by an Extra-Amygdala Septohypothalamic Circuit. *Cell*. 2014 Jan;156(3):522–36. [PubMed: 24485458]
61. Sweeney P, Yang Y. An Inhibitory Septum to Lateral Hypothalamus Circuit That Suppresses Feeding. *J Neurosci*. 2016 Nov 2;36(44):11185–95. [PubMed: 27807162]
62. Siehler S, Hoyer D. Characterisation of human recombinant somatostatin receptors. 4. Modulation of phospholipase C activity. *Naunyn-Schmiedeberg's Archives of Pharmacology*. 1999 Nov 4;360(5):522–32. [PubMed: 10598791]
63. Fehlmann D, Langenegger D, Schuepbach E, Siehler S, Feuerbach D, Hoyer D. Distribution and characterisation of somatostatin receptor mRNA and binding sites in the brain and periphery. *Journal of Physiology-Paris*. 2000 Oct;94(3–4):265–81. [PubMed: 11088004]

64. Ramírez JL, Mouchantaf R, Kumar U, Otero Corchon V, Rubinstein M, Low MJ, et al. Brain Somatostatin Receptors Are Up-Regulated In Somatostatin-Deficient Mice. *Molecular Endocrinology*. 2002 Aug 1;16(8):1951–63. [PubMed: 12145348]
65. Stengel A, Karasawa H, Taché Y. The role of brain somatostatin receptor 2 in the regulation of feeding and drinking behavior. *Hormones and Behavior*. 2015 Jul;73:15–22. [PubMed: 26026616]

Author Manuscript

Author Manuscript

Author Manuscript

Author Manuscript

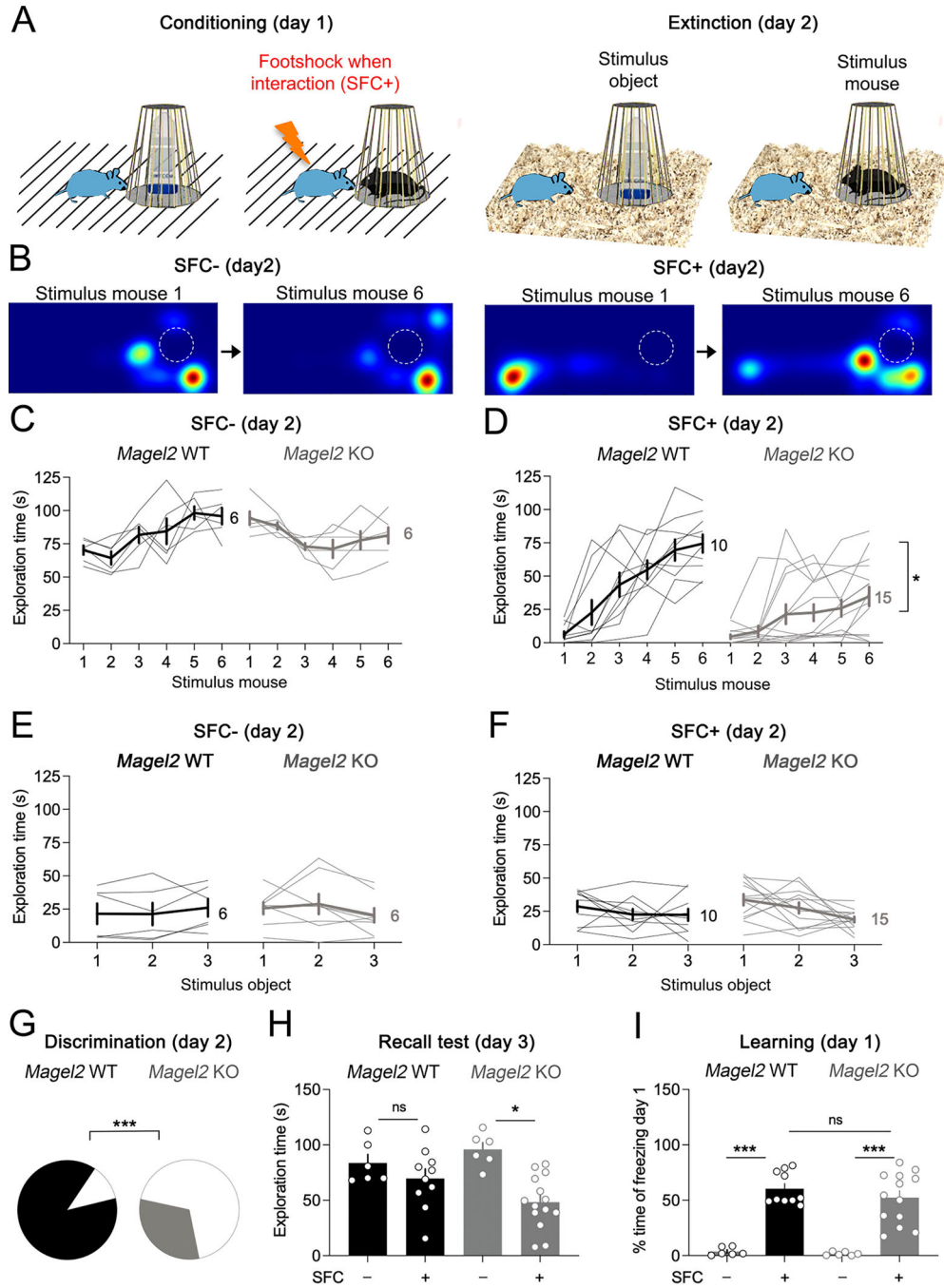


Figure 1. *Magel2*KO mice exhibit social-fear extinction deficits

(A) Social-fear conditioning (SFC) on day 1 is followed by extinction learning protocol in homecage, 24 hours later, on day 2.

(B) Heatmaps of the time exploring stimulus mice in homecage during extinction trial 1 and 6 on day 2. The dashed circle represents the stimulus box holding the stimulus mice.

(C) Time exploring stimulus mice on day 2 if no electric footshock was applied on day 1 (SFC-). Bold lines indicate means±SEM, light lines individual subjects (N). Two-way

ANOVA: Effect of trials \times genotype $F_{(5,50)}=7$ $p<0.0001$, effect of genotype $F_{(1,10)}=0.1$ $p=0.7$, effect of trials $F_{(5,50)}=2$ $p=0.12$.

(D) Time exploring stimulus mice on day 2 if at least one footshock was applied when exploring the stimulus mouse on day 1 (SFC+). Two-way ANOVA: Effect of trials \times genotype $F_{(5,115)}=5.1$ $p=0.0003$, effect of genotype $F_{(1,23)}=13.9$ $p=0.001$, effect of trials $F_{(2,7,62)}=28.5$ $p<0.0001$. Bold lines indicate means \pm SEM, light lines individual subjects (N).

(E) Time exploring stimulus objects on day 2 of the SFC- group. Bold lines indicate means \pm SEM, light lines individual subjects (N). Two-way ANOVA: Effect of trials \times genotype $F_{(2,24)}=2.8$ $p=0.17$, effect of genotype $F_{(1,12)}=0.005$ $p=0.08$, effect of trials $F_{(2,24)}=0.15$ $p=0.08$.

(F) Time exploring stimulus objects on day 2 of the SFC+ group. Bold lines indicate means \pm SEM, light lines individual subjects (N). Two-way ANOVA: Effect of trials \times genotype $F_{(2,42)}=0.8$ $p=0.4$, effect of genotype $F_{(1,21)}=0.3$ $p=0.5$, effect of trials $F_{(2,42)}=4.3$ $p=0.02$.

(G) Proportion of mice discriminating between the stimulus mice by 20% of exploration time (Chi^2 $p<0.0001$).

(H) Time exploring a novel stimulus mouse on day 3, to test recall of extinction memory (means \pm SEM). Two-way ANOVA: Effect of SFC \times genotype $F_{(1,32)}=4.2$ $p=0.04$, effect of genotype $F_{(1,32)}=0.32$ $p=0.5$, effect of SFC $F_{(1,32)}=14.1$ $p=0.0007$. Post-hoc Tukey's test, * $p=0.001$.

(I) Time of freezing immediately post-conditioning (means \pm SEM). Two-way ANOVA: Effect of SFC \times genotype $F_{(1,31)}=0.2$ $p=0.6$, effect of genotype $F_{(1,31)}=0.7$ $p=0.4$, effect of SFC $F_{(1,31)}=83.4$ $p<0.0001$. Post-hoc Tukey's test, *** $p<0.0001$.

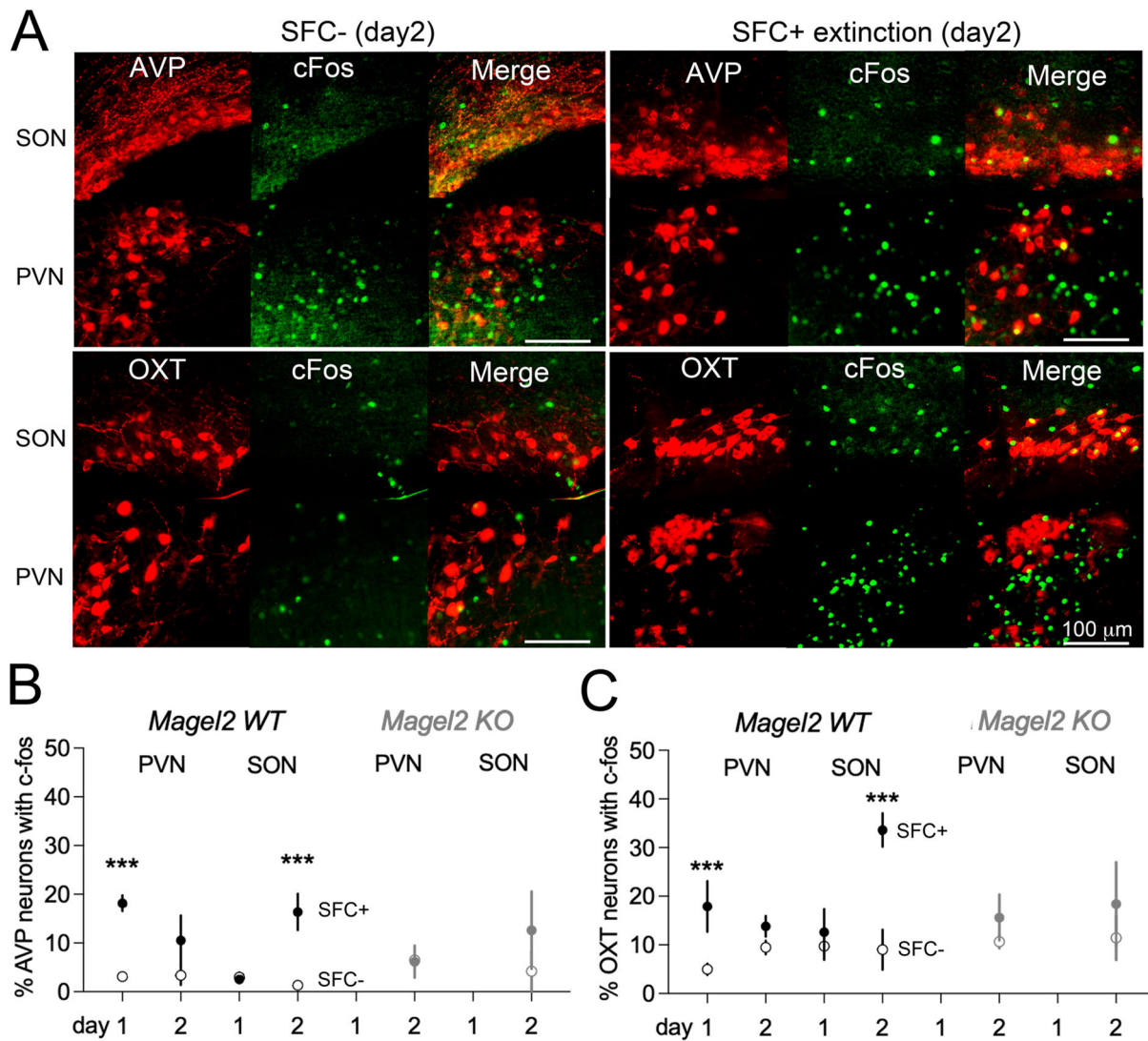


Figure 2. Differential activation of hypothalamic neurons during the acquisition and extinction of SFC, and in *Magel2*KO mice

(A) Co-staining with c-Fos and neurophysin antibodies in brain sections harvested 60 min after extinction in *Magel2*WT mice.

(B) Number of Fos-activated AVP neurons engaged by behavior. Data are means \pm SEM in N 4 mice/group. Comparison between groups with Mann-Whitney test as indicated.

(C) Number of Fos-activated OXT neurons engaged by behavior. Data are means \pm SEM in N 4 mice/group. Comparison between groups with Mann-Whitney test as indicated.

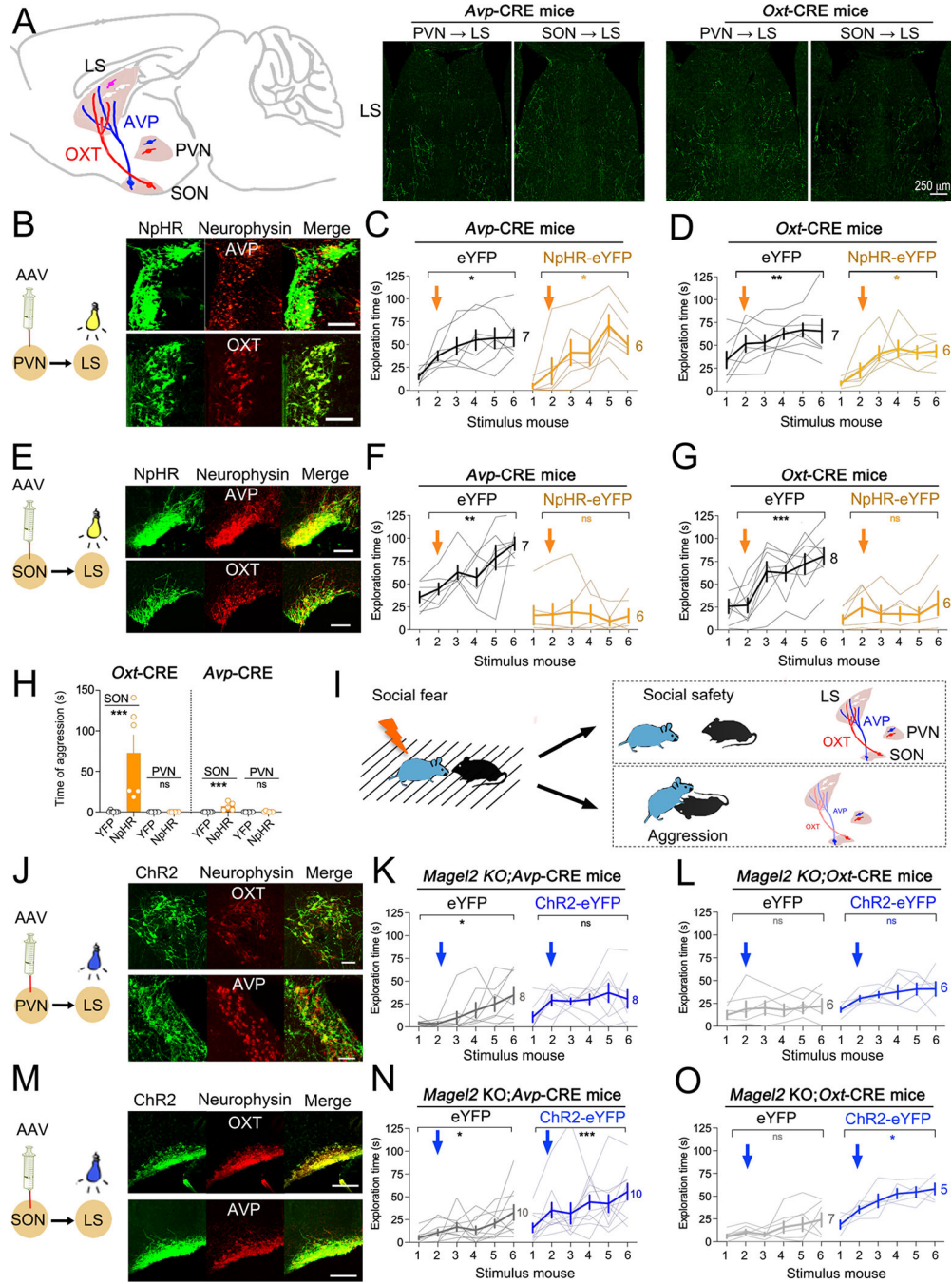


Figure 3. Pathway-specific control of social-fear extinction impaired in *Magel2*KO mice
 (A) Hypothalamo-septal pathways. Coronal sections showing projections in the LS from neurons targeted with AAV encoding CRE-dependent eYFP in *Avp*-CRE and *Oxt*-CRE mice.
 (B) Specificity of transgene expression in *Avp*-CRE and *Oxt*-CRE mice. Scale=40 μ m.
 (C) Optogenetic inhibition of the PVN→LS pathway in AVP neurons had no effect. Arrows mark the onset of laser stimulation. Bold lines are means±SEM, light lines individual subjects (N). Two-way ANOVA: effect of trials $F_{(2,6,29)}=16.5$ $p<0.0001$ post-hoc Sidak test.

- (D) Optogenetic inhibition of the PVN→LS pathway in OXT neurons had no effect. Two-way ANOVA: effect of trials $F_{(2.4,26)}=11.3$ $p=0.0001$. Post-hoc analysis with Dunnett test.
- (E) Specificity of transgene expression in *Avp*-CRE and *Oxt*-CRE mice. Scale=40 μ m.
- (F) Optogenetic inhibition of the SON→LS pathway in AVP neurons impaired SFC extinction. Two-way ANOVA: effect of NpHR $F_{(1,11)}=27.1$ $p=0.0003$; trials \times NpHR $F_{(5,55)}=4.7$ $p=0.0012$ post-hoc Sidak test.
- (G) Optogenetic inhibition of the SON→LS pathway in OXT neurons impaired SFC extinction. Two-way ANOVA: effect of NpHR $F_{(1,12)}=10.5$ $p=0.007$; trials \times NpHR $F_{(5,60)}=7.1$ $p<0.0001$ post-hoc Sidak test.
- (H) Cumulated time of attacks on the 6 stimulus mice (means \pm SEM, N mice as indicated). Comparison between groups with Mann Whitney test: YFP vs NpHR in SON OXT neurons $p=0.0012$ and in SON AVP neurons $p=0.0013$.
- (I) Model: loss of OXT in the SON→LS pathway prevented social-fear extinction and promoted aggressive behavior. Loss of AVP in this pathway did not completely overlap with that of OXT.
- (J) Specificity of transgene expression in *Mage12*KO crossed with *Avp*-CRE and *Oxt*-CRE mice. Scale=40 μ m.
- (K) Optogenetic activation of the PVN→LS pathway in AVP neurons had no effect. Two-way ANOVA: effect of trials $F_{(2.8,39.9)}=4.9$ $p=0.006$ post-hoc Sidak test.
- (L) Optogenetic activation of the PVN→LS pathway in OXT neurons had no effect. Two-way ANOVA: effect of trials $F_{(3.1,31.5)}=3.7$ $p=0.018$ post-hoc Sidak test.
- (M) Specificity of transgene expression in *Mage12*KO crossed with *Avp*-CRE or *Oxt*-CRE mice. Scale=10 μ m.
- (N) Optogenetic activation of the SON→LS pathway in AVP neurons promoted SFC extinction in *Mage12*KO mice. Two-way ANOVA: effect of Chr2 $F_{(1,11)}=8.8$ $p=0.01$ post-hoc Sidak test.
- (O) Optogenetic activation of the PVN→LS pathways in OXT neurons promoted SFC extinction in *Mage12*KO mice. Two-way ANOVA: effect of Chr2 $F_{(1,10)}=37.65$ $p=0.003$ post-hoc Sidak test.

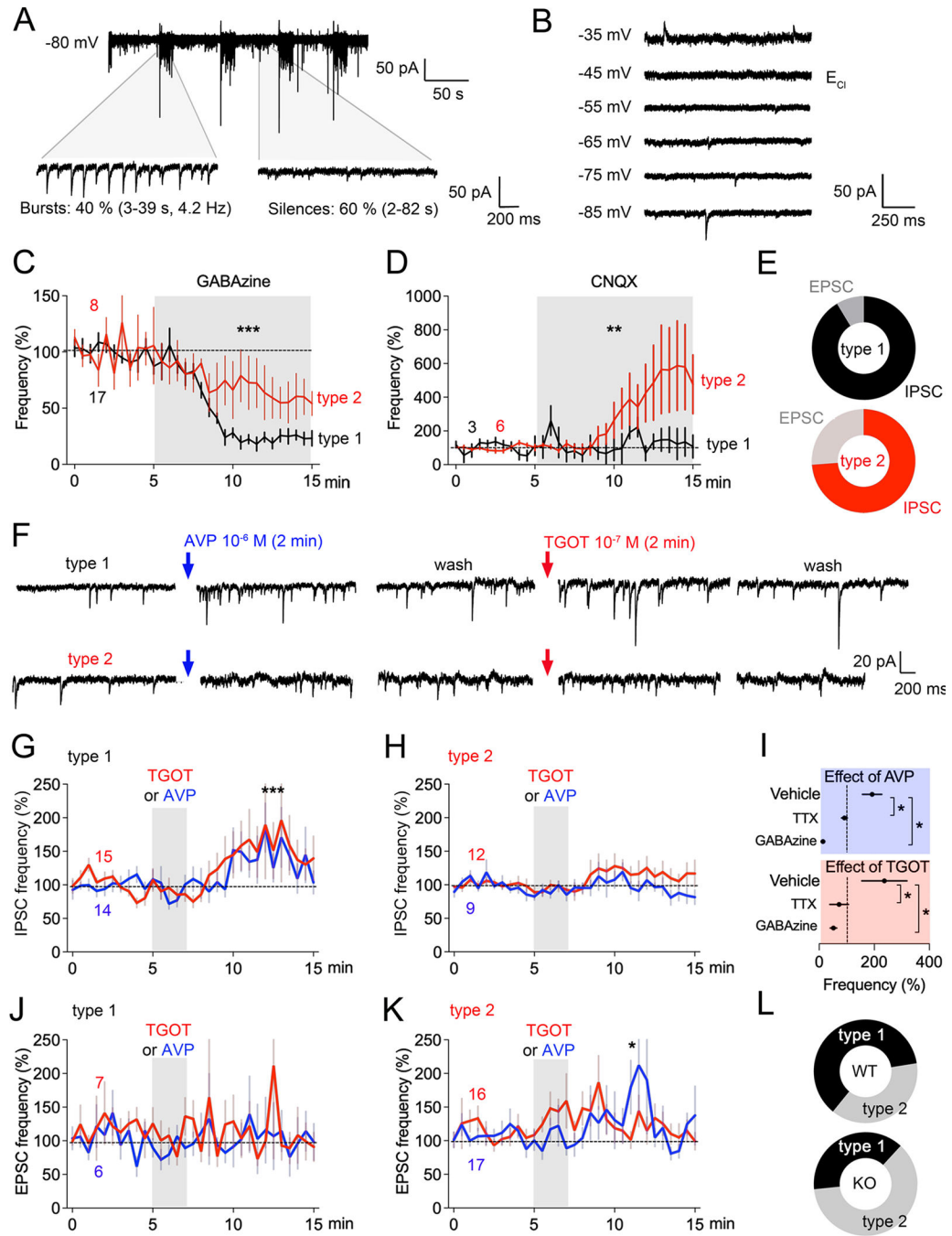


Figure 4. Modulation of inhibitory synaptic transmission by TGOT and AVP is impaired in the LS of *Magel2*KO mice

(A) Synaptic events recorded at -80 mV with patch clamp in slices of LS show bursting activity. (B) Depolarization steps suppressed a majority of synaptic events when reaching the inversion potential of GABAergic currents set at $E_{Cl} = -45$ mV.

(C) GABAazine (0.3 μ M) distinguished two types of responses: the near full inhibition (73 \pm 5% N=12, type-1) and the partial (41 \pm 12% N=5, type-2). Type-1 is the most represented with 70% of all cells recorded in the LS (N=61). Means \pm SEM, two-way

ANOVA: effect of GABAzine $F_{(30,666)}=9$ $p<0.0001$; GABAzine \times cell type $F_{(30,666)}=1.77$ $p=0.008$ post-hoc Sidak test.

(D) Bursting synaptic events are still observed after inhibition of glutamatergic currents with CNQX (1 μ M). Means \pm SEM, two-way ANOVA: difference between cell types $F_{(1,216)}=13.3$ $p=0.0003$.

(E) Proportion of excitatory currents is higher than inhibitory currents in the type-2 cells unlike in the type-1 cells.

(F) Modulation of synaptic events in type-1 cells by 1 μ M AVP and 0.1 μ M TGOT for 2 min.

(G) Frequency of IPSC in type-2 cells modulated by AVP and TGOT (Means \pm SEM).

Kruskal Wallis test comparing before and after stimulation $p=0.0004$ for TGOT and $p=0.03$ for AVP.

(H) No effect of AVP and TGOT on the frequency of IPSC in type-1 cells (Means \pm SEM).

(I) TTX (0.3 μ M) and GABAzine (0.3 μ M) blocked AVP response and TGOT response in type-1 cells (Means \pm SEM, paired t-test $p<0.03$).

(J) No effect of AVP and TGOT on the frequency of EPSC in type-1 cells (Means \pm SEM).

(K) Effect of AVP on the frequency of EPSC in type-2 cells (Means \pm SEM). Kruskal Wallis test comparing before and after stimulation $p=0.012$.

(L) Less type-1 than type-2 cells in *Magel2*KO mice (N=52 cells) compared to *Magel2*WT controls (N=60 cells). Chi^2 $p<0.0001$.

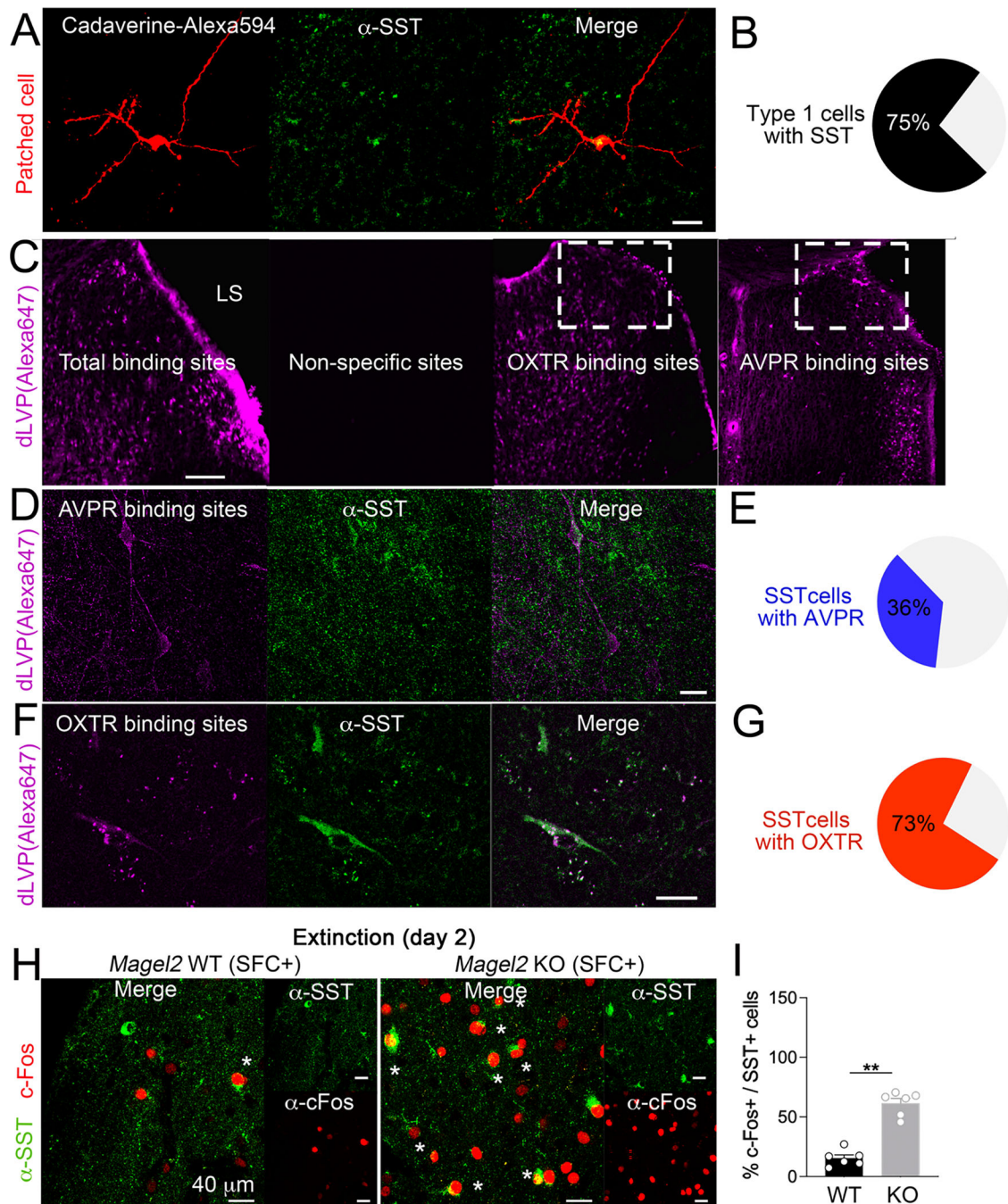


Figure 5. LS neurons modulated by TGOT and AVP are somatostatinergic, and more engaged by social-fear extinction in *Magel2*KO mice than in WT controls

(A) Infusion of Cadaverine dye in the patch pipette labeled type-1 cells counterstained with somatostatin (SST) antibodies. Scale=25 μ m.

(B) Proportion of type-1 cells (N=16) with SST marker. Scale=200 μ m.

(C) Binding specificity of the fluorescent peptide: 50 μ M d[Lys(Alexa-647)⁸]VP without (total binding) or with 100 μ M Manning compound (non-specific). OXTR binding sites marked with 10 μ M d[Lys(Alexa-647)⁸]VP when AVPR were saturated with 5 μ M of the competitive ligand Manning compound. AVPR binding sites marked with 50 μ M

d[Lys(Alexa-647)⁸]VP when OXTR were saturated with 5 μ M of the competitive ligand TGOT.

(D) AVPR binding counter-stained with SST antibodies in dLS. Scale=25 μ m.

(E) A minority of SST-neurons in dLS (N=203) co-express AVPR binding sites.

(F) OXTR binding counter-stained with SST antibodies in dLS. Scale=25 μ m.

(G) A majority of SST-neurons in dLS (N=265) co-express OXTR binding sites.

(H) Co-staining with c-Fos and SST antibodies in dLS of *Mage12*KO mice and WT-controls sacrificed 1h after social-fear extinction.

(I) Proportion of SST-neurons co-labeled with c-Fos in LS. Data are means \pm SEM in N=6 mice/group. Mann-Whitney test $p<0.05$.

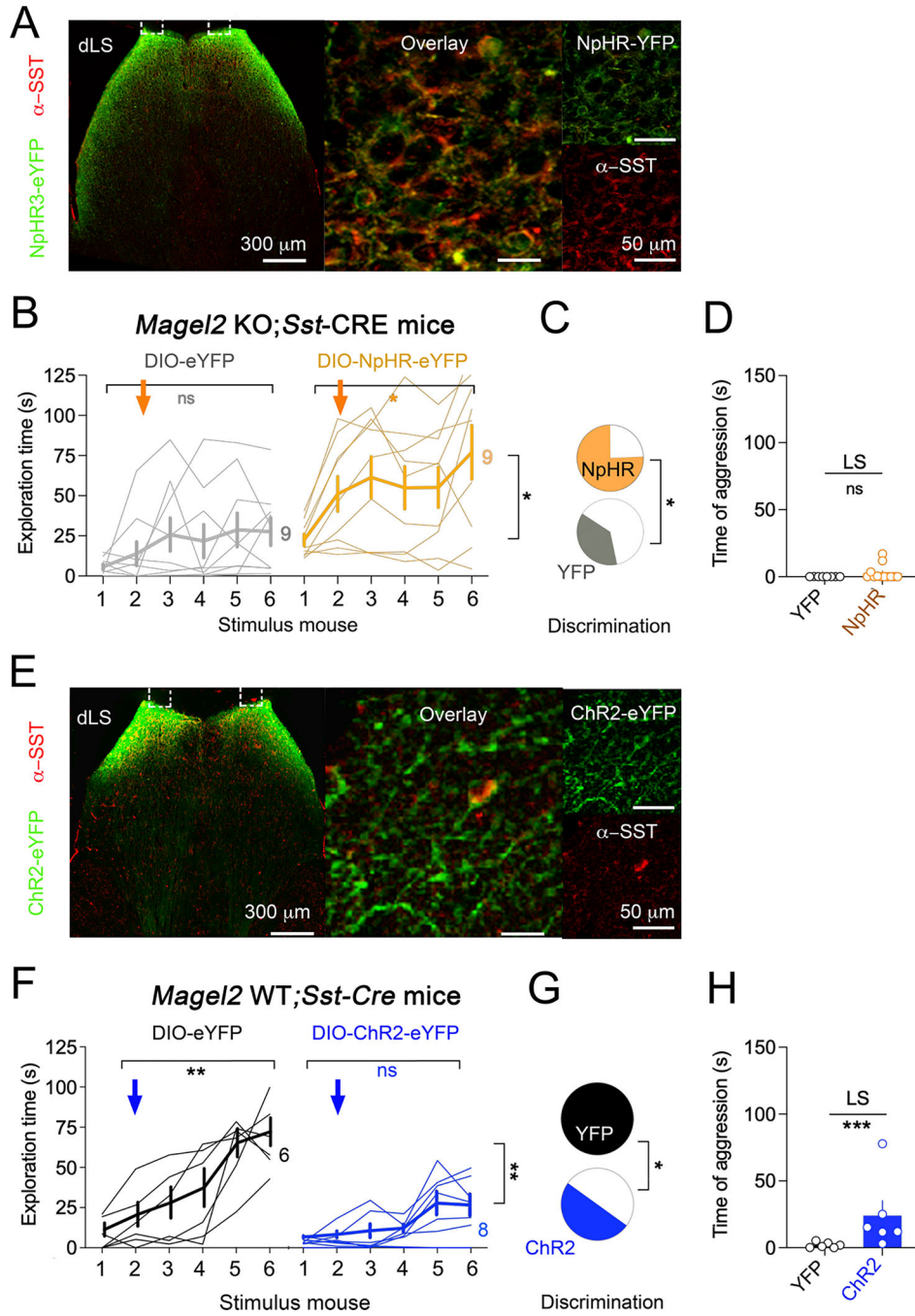


Figure 6. Inhibition of SST-neurons in LS ameliorates social-fear extinction deficits of *Magel2*KO mice whereas hyperactivation causes aggression

(A) Expression of CRE-dependent transgene in LS of *Magel2*KO crossed with *Sst*-CRE mice.

(B) Optogenetic inhibition of LS SST-neurons prevented social-fear extinction deficits in *Magel2*KO mice. Arrows mark the onset of continuous yellow light stimulation. Bold lines are means±SEM, light lines individual subjects (N). Two-way ANOVA: Effect of NpHR3 versus YFP $F_{(1,19)}=17.2$ $p=0.0005$; interaction of time × NpHR3 $F_{(4,76)}=9.6$ $p<0.0001$ post-hoc Sidak test.

- (C) Discrimination between stimulus mice during extinction increased in NpHR3 KO group compared to YFP KO-controls ($\text{Chi}^2 p=0.01$).
- (D) Cumulated time of attacks on the 6 stimulus mice was not affected by silencing of LS SST-neurons in *Mage12*KO mice (means \pm SEM).
- (E) Expression of CRE-dependent transgene in LS of *Mage12*WT crossed with *Sst*-CRE mice.
- (F) Optogenetic activation of LS SST-neurons impaired social-fear extinction in WT-controls. Arrows mark the onset of pulsed blue light stimulation. Bold lines are means \pm SEM, light lines individual subjects (N). Two-way ANOVA: Effect of ChR2 versus YFP $F_{(1,12)}=14.6 p=0.002$; interaction of trials \times ChR2 $F_{(5,59)}=5.1 p=0.0006$ post-hoc Sidak test.
- (G) Discrimination between stimulus mice during extinction increased in ChR2 group compared to YFP WT-controls ($\text{Chi}^2 p<0.05$).
- (H) Cumulated time of attacks on the 6 stimulus mice increased with optogenetic stimulation of LS SST-neurons (means \pm SEM). Mann Whitney test comparing ChR2 and YFP groups $p=0.0087$.

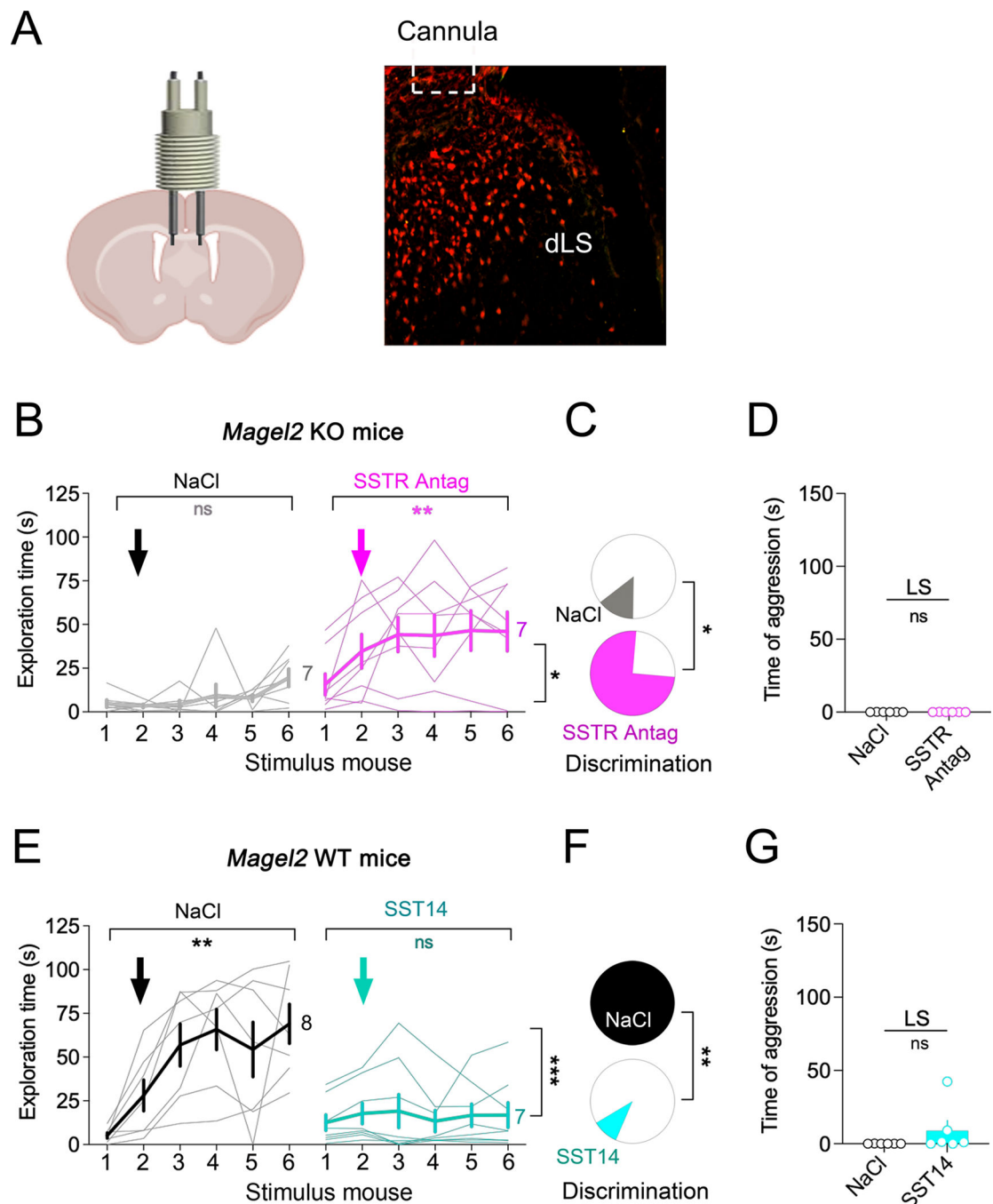


Figure 7. SSTR in LS are required for social-fear extinction but not aggression
 (A) Diffusion area in dLS of a fluorescent tracer injected through a cannula.
 (B) Injection of the SSTR pan-antagonist cyclosomatostatin (2 $\mu\text{g}/\text{side}$ (62,63)) in LS improved social-fear extinction deficits of *Magel2*KO mice. Arrows indicate the onset of injection. Bold lines are means \pm SEM, light line individual subjects (N). Two-way ANOVA: time \times SSTR antagonism $F_{(4,55)}=2.7$ $p=0.03$ post-hoc Sidak test.
 (C) Discrimination between stimulus mice during extinction increased with cyclosomatostatin compared to NaCl-injected KO-controls (Chi^2 $p=0.001$).

(D) Cumulated time of attacks on the 6 stimulus mice not affected by cyclosomatostatin in LS (means±SEM). Mann Whitney test comparing antagonist and vehicle groups $p=0.3$.

(E) Injection of the SSTR agonist SST14 (1 ng/side, (64,65)) in LS impaired social-fear extinction of *Magel2*WT mice. Arrows indicate the onset of injection. Bold lines are means±SEM, light line individual subjects (N). Two-way ANOVA: time × SST $F_{(4,50)}=4$ $p=0.006$ post-hoc Sidak test.

(F) Discrimination between stimulus mice decreased with SST14 compared to NaCl-injected WT-controls (Chi² $p=0.002$).

(G) Cumulated time of attacks on the 6 stimulus mice not affected by SST14 in LS (means±SEM). Mann Whitney test comparing SST14 and NaCl groups $p=0.06$ (non-significant trend).

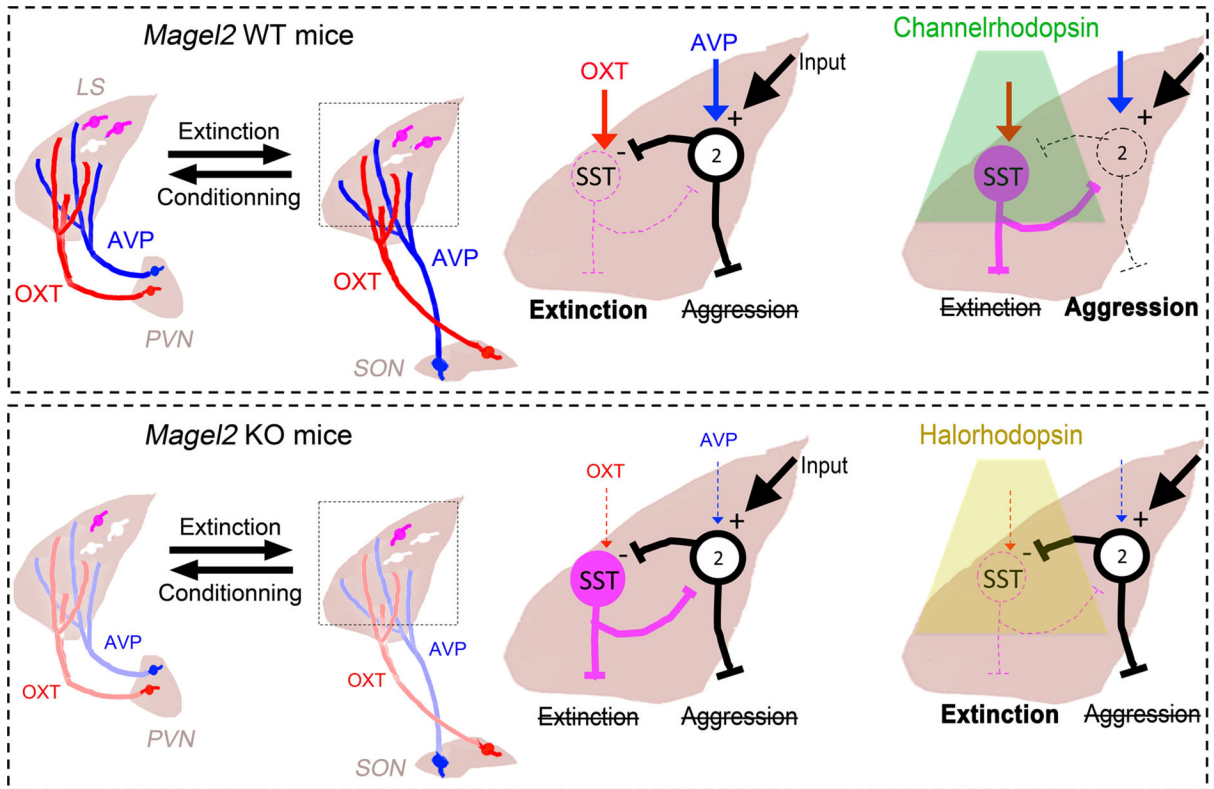


Figure 8. A proposed ‘functional unit’ in LS consisting of SST-neurons, which regulates the balance between social-fear extinction and social aggression in *Magel2*KO mice. In WT mice, inhibition of SST cells by OXT (type-1 cells) and by AVP-responsive type-2 cells (together forming the functional unit) disinhibits social-fear extinction circuits, while suppressing aggression (*Top, left*). Activating SST cells with channelrhodopsin suppresses fear extinction, while simultaneously disinhibiting aggression circuits (*Top, right*). Weakening of OXT and AVP inputs from supraoptic nucleus in *Magel2*KO mice strengthens activity of both sub-units and therefore bolsters inhibitory effects of the functional unit as a whole. As a result, social-fear extinction and aggression are both suppressed (*Bottom, left*). Reversing this by selectively inhibiting SST cells with halorhodopsin disinhibits and enables social-fear extinction, while in the other arm of the unit aggression still remains inhibited (*Bottom, right*).